Supplementary Methods

Cell lines. A HPF cell line was obtained from ScienceCell Research Laboratories. I90 was donated by Ben Yu's (UCSD) laboratory. HPF and FLS were cultured in DMEM supplemented with 10% FBS, glutamine and antibiotics lacking added pyruvate. In glucose deprivation experiments, cells were cultured with DMEM complemented with dialyzed serum.

Lactate and glucose profiling using ^{1}HMRS. RA and OA FLS and synovium were isolated and prepared for ^{1}HMRS analyses as described (1, 2). MRS spectra were acquired at 16.4 T (700 MHz) on a Bruker Avance spectrometer (Bruker BioSpin Corp., Billerica, MA, USA) equipped with a TCI cryoprobe and high-throughput robotics. One-dimensional ^{1}HMRS spectra were acquired using at least 512 scans and 8 dummy scans, 32K data points, and a spectral width of 9.8 kHz. Excitation sculpting pulse sequence was implemented to suppress the water signal. All the MRS datasets were processed using MetaboLab in the MATLAB programming environment (MathWorks, Inc., Natick, MA) (3). MRS spectra were normalized based on the probabilistic quotient normalization method (4). Assignment of MRS resonances and metabolite quantification were performed using Chenomx NMR Suite and other available databases (5, 6)

Immunohistochemistry. Paraffin sections prepared from arthritic mouse joints, were incubated overnight at 4°C with mouse anti-human GLUT1 antibody (Sigma-Aldrich Co) at a 1:200 dilution. Citrate buffer was used at 42°C overnight for antigen retrieval. The signal was developed using diaminobenzidine and sections were counterstained with hematoxylin.

Measurement of O_2 and H^+ flux: Analysis of intact FLS oxygen consumption and proton production rates were conducted using Seahorse technology in XF96-well plates (7) and interpreted as previously described (8). Cells were plated at 15,000/well in growth medium, LPS was added the following day and measurements were made 24 hrs later. On the day of assay, growth medium was removed, and replaced with assay medium comprising unbuffered DMEM with 10 mM glucose, 3 mM glutamine, and 1mM pyruvate (pH 7.4 at 37°C). Rates of endogenous respiration were first measured, followed by addition of 2 μM oligomycin. The difference between these two rates is indicative of the rate of ATP turnover (ATP-linked respiration). Next, 400 nM FCCP was added (the concentration was optimized in preliminary studies) to measure the maximal rates at which the electron transport chain and oxidative metabolic pathways can function, followed by rotenone (2 μM) and antimycin A (1 μM) to measure non-mitochondrial oxygen consumption. Extracellular acidification rates (mpH/min) were converted to proton production rates by calculating the buffer capacity for the assay medium in the 2.28 μL XF96 microchamber as described in (7). Permeabilized cell respiration was conducted as previously described (7) in assay buffer containing 70 mM sucrose, 220 mM mannitol,10 mM KH_2PO_4, 5 mM $MgCl_2$, 2 mM HEPES, 1 mM EGTA, 0.2% (w/v) fatty acid-free BSA, 4 mM ADP, 3 nM recombinant perfringolysin O (XF-PMP, Seahorse Biosciences) supplemented with either 10 mM succinate plus 2 μM rotenone, or 5 mM pyruvate plus 1 mM malate (pH 7.2 at 37°C). Following addition of 2 μM oligomycin, maximal respiration was determined by adding sequential pulses of 2 μM FCCP followed by rotenone (2 μM) and antimycin A (1 μM).

WB analysis. FLS were disrupted in lysis buffer (PhosphoSafe™ , Novagen, Gibbstown, NJ). Proteins were separated by SDS-PAGE and transferred to a nitrocellulose

membrane. Blots were probed with antibodies against subunits of electron transport chain complexes (Life Technologies Anti-OxPhos Complex Kit #457999), GLUT1 (Santa Cruz, Co), p-AKT(thr308), p-AKT(ser473) and total AKT (Cell Signaling Technology, Danvers, MA) and actin (Sigma-Aldrich, Co) at 1:1000 dlution. Horseradish peroxidase-conjugated anti-IgG (Cell Signaling Technology, Danvers, MA) was used as secondary antibody at 1:2000 dilution. Membranes were developed using a chemiluminescence system (ECL detection reagent: Amersham Life Science, Aylesbury, UK).

Real-time quantitative PCR (qPCR). FLS were collected and total RNA was extracted with Trizol (Invitrogen). RNA was quantified and assessed for purity using a NanoDrop spectrophotometer (Rockland, DE, USA). RNA integrity was verified with a BioAnalyzer 2100 (Agilent, Palo Alto, CA, USA). Total RNA 200 ng from each sample was used for cDNA synthesis using the Superscript II kit (Invitrogen). qPCR was performed with SYBR Green PCR Master Mix Kit (Applied Biosystems, Foster City, CA). The relative amounts of transcripts were compared to those of HRPT and normalized to untreated samples by the $^{\Delta\Delta}$Ct method. Primers are available upon request.

Lactate and glucose measurement. Media samples after 24 hrs of LPS stimulation were collected and stored at -20C until the time of the assay. Glucose assay kit (Cayman Chemical) and L-lactate assay kit (Eton Bioscience) were measured in the conditioned media of cell incubations using colorimetric kits according to manufacturer's instructions

Purine nucleotide synthesis. Cells in six-well dishes were incubated for 2 h with 10 μCi of ^{14}Cformate (54 mCi/mmol, final concentration 185 μM). They were washed with ice-cold PBS, and extracted *in situ* in 0.4 N perchloric acid (8, 9). The extracts were heated to 100□C for 70 min to break the N-glycosidic bond between the purine base and ribose

group. The samples were centrifuged at 1000 *g* for 5 min, and supernatants were applied to AG Dowex 50 columns, which were washed with 0.1 N HCl to remove unreacted formate and other anions. Purines were eluted in 6 N HCl and radioactivity was measured.

Glucose oxidation. Carbon flow through the oxidative branch of the pentose phosphate pathway was measured by following CO_2 release from [1-^{14}C] glucose oxidation as described previously (10). Briefly, cells were incubated in 25 cm^2 flasks in DMEM containing 10% dialyzed FBS. The flasks were capped tightly with a rubber septum that held a plastic center well (Kontes Glass Co.) containing a fluted piece of Whatman No. 1 filter paper. The cells were incubated for 1 h with 1 μCi of [1-^{14}C] glucose (specific activity, 55 mCi/mmol). At the end of the incubation, the center well and the filter paper were saturated with 1 N NaOH and radioactive CO_2 was trapped in the NaOH, and was measured by liquid scintillation counting.

ELISA. IL-1β, IL-6 from joint extract and IL-6 and MMP3 from FLS supernatants were evaluated by DuoSet enzyme-linked immunosorbent assay following the manufacturer's protocol.

MTT assay. For the MTT assay, 3×10^3 FLS/well were plated into 96-well plates in 10% FBS/DMEM. After 24 hours, the medium was replaced with low-serum medium (0.1% FBS/DMEM) for 24 hours for synchronization. On day 0, medium was replaced with 1% FBS and cells were treated with BrPa (25uM), 2DG (50mM) or medium without glucose. PDGF or medium alone was added to the appropriate wells. The experiment was performed in triplicate wells. Cell viability was estimated on day 4 after incubation with MTT for 4 hours and was read at 550 nm with a spectrophotometer.

Migration scratch assay. FLS were seeded onto 24-well plates and allowed to come to confluence. Cells were incubated with BrPa (25uM), 2DG (50mM), 0.1% FBS, or medium without glucose. A single scratch wound was induced through the middle of each well with a sterile pipette tip. Cells were subsequently exposed to PDGF (10ng/ml) for 36 hrs. FLS were fixed with buffered formalin 10%. Violet crystal was used at a a concentration of 0.05% in distilled water for 30 minutes. After staining cells were washed with tap water for 15 minutes and FLS migration across the wound margins was assessed, photographed and measured by ImageJ as the average of relative area between margins in 4 different fields at 36hrs.

Histology analysis. Joints were fixed in 10% formalin, decalcified in 10% EDTA for 2-3 weeks and paraffin embedded. Sections were prepared from the tissue blocks and stained with hematoxylin and eosin (H&E) and safranin O. A blinded semiquantitative scoring system was used to assess synovial inflammation, extra-articular inflammation, bone erosion and cartilage damage (0-5 scale), as previously described (11).

Supplementary Figure 1

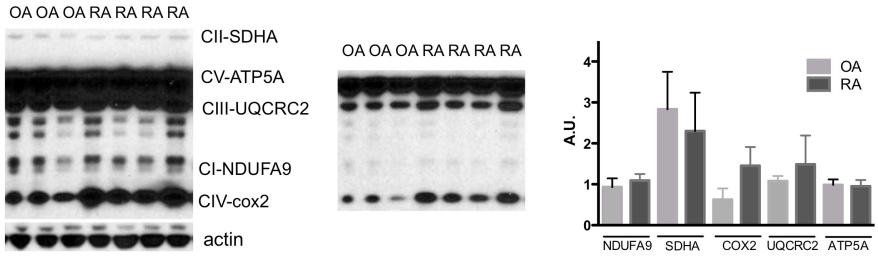

Supplementary Figure 1. Mitochondrial complexes in RA and OA cell lines. Expression levels of components of the electron transport chain complexes were determined by WB in RA and OA FLS cell lines. Semi-quantitative densitometry analysis of Western blots (arbitrary densitometry units) of indicated proteins in is shown. Expression of the different components of the mitochondrial complexes was not different between FLS cell lines.

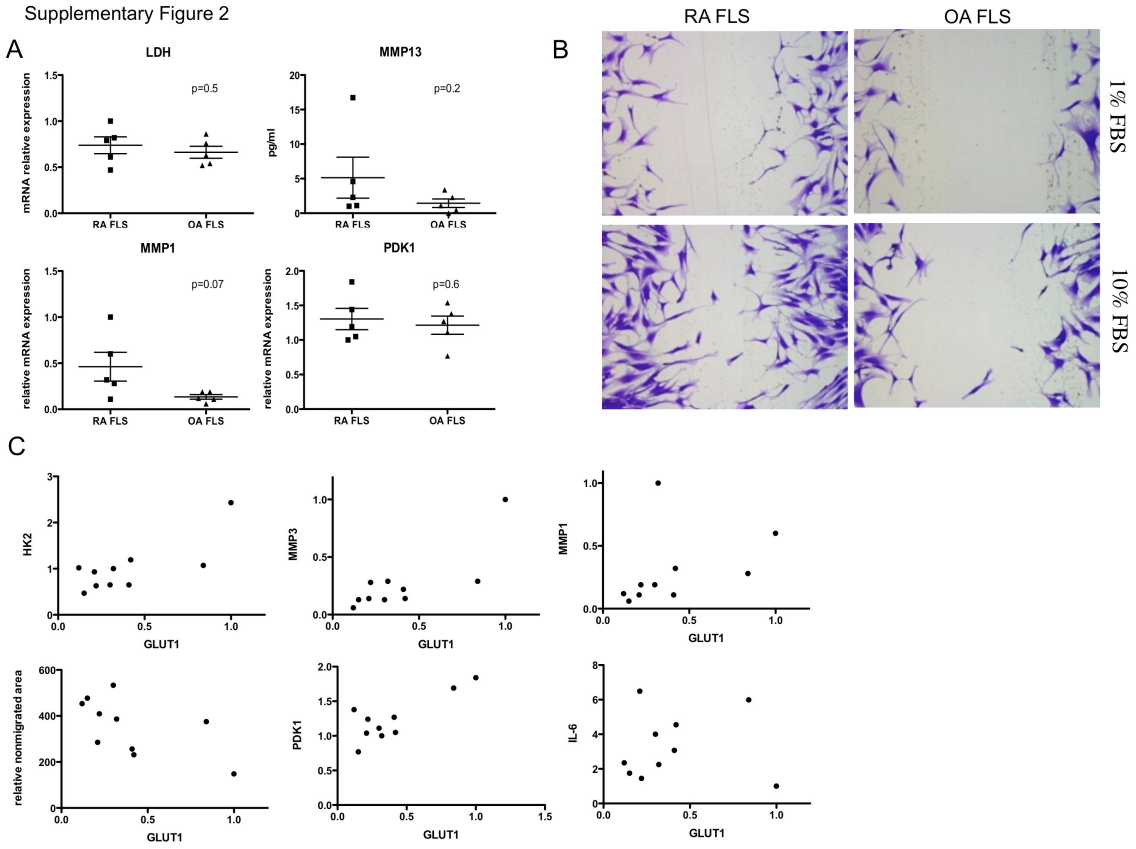

Supplementary Figure 2. GLUT1 expression correlates with glycolytic genes. **(A)** Expression of select genes by qPCR in 5 RA and 5 OA cell lines are plotted. **(B)** Representative images of one RA and OA FLS in the migration scratch assay after crystal violet staining. **(C)** Scatterplot graphics of the correlations for HK2, MMP1, MMP3, migration, PDK1 and IL6 with GLUT1.

Supplementary Figure 3

A

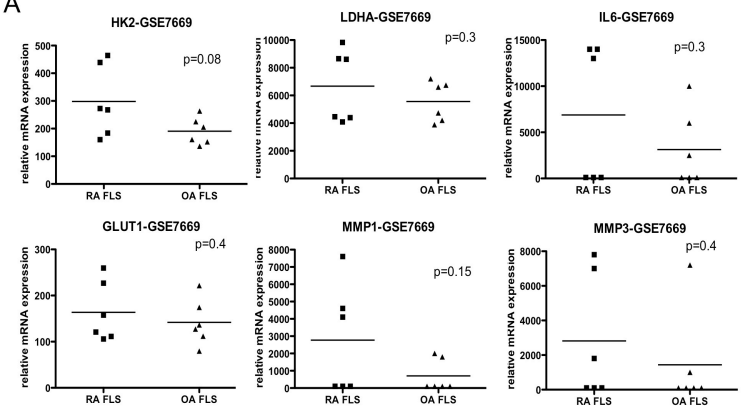

B

	GLUT1 (p)	Pearson r
HK2	0.02	0.65
Pdk1	0.018	0.66
LDHA	0.004	0.75
IL-6	0.022	0.65
CSF1	0.1	0.51
MMP1	0.0065	0.73
MMP3	0.0062	0.73

Supplementary Figure 3. GLUT1 expression correlates with glycolytic genes. **(A)** Baseline expression of several genes in RA and OA FLS from GSE7669 array (http://www.ncbi.nlm.nih.gov/sites/GDSbrowser?acc=GDS2931) **(B)** Correlations of the previous genes with GLUT1 expression are shown.

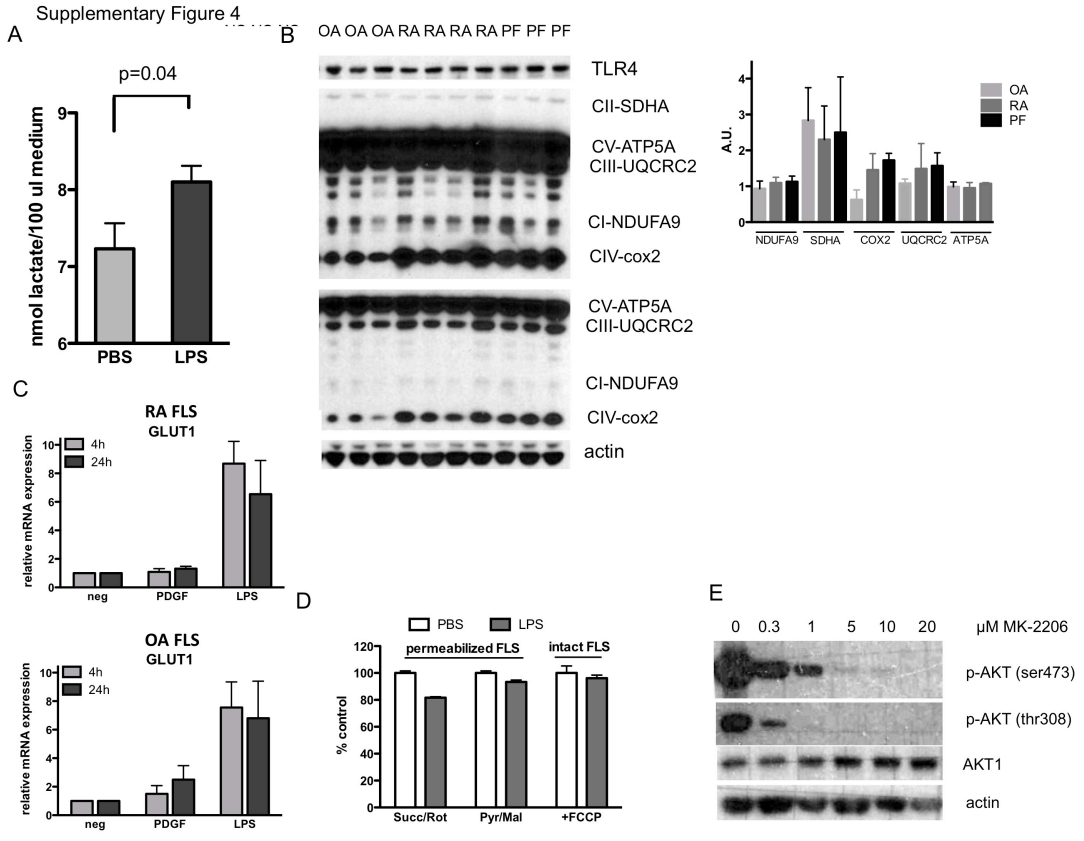

Supplementary Figure 4. **OA FLS cell lines behave similar to RA FLS after stimulation** (A) L-Lactate from supernatants of cultured OA FLS after LPS (1µg/ml) stimulation was measured as described in Methods**. (B)** TLR4 expression and electron transport chain subunits were determined by WB in RA, OA and PF (extended WB from Supplementary Figure 1). Semi-quantitative densitometry analysis of Western blots (arbitrary densitometry units) of indicated proteins is shown. Expression of the different components of the mitochondrial complexes was not different between cell lines. **(C)** RA FLS (upper panel) and OA FLS (lower panel) were stimulated with different stimuli (PDGF 10ng/ml, LPS 1µg/ml) for 4 and 24hrs, and GLUT1 expression was determined my qPCR. Data are pooled from three different cell lines. Data are presented as mean±S.E.M. **(D)** 3 OA cell lines were incubated for 24 hours with LPS (1mg/ml).

Permeabilized cell respiration was then measured as described in the Methods with either succinate (plus rotenone) or pyruvate (plus malate) as substrates (left bars). The right bar is the pooled rate of uncoupler-stimulated respiration of 3 intact OA cells lines, following 24 hour exposure to LPS. **(E)** RA FLS cell line was first incubated with an AKT inhibitor (MK-2206, 5μM) at different concentrations for one hour and then stimulated with TNF (10ng/ml) for 15 minutes. P-AKT, AKT and actin expression was determined my WB.

Supplementary Figure 5

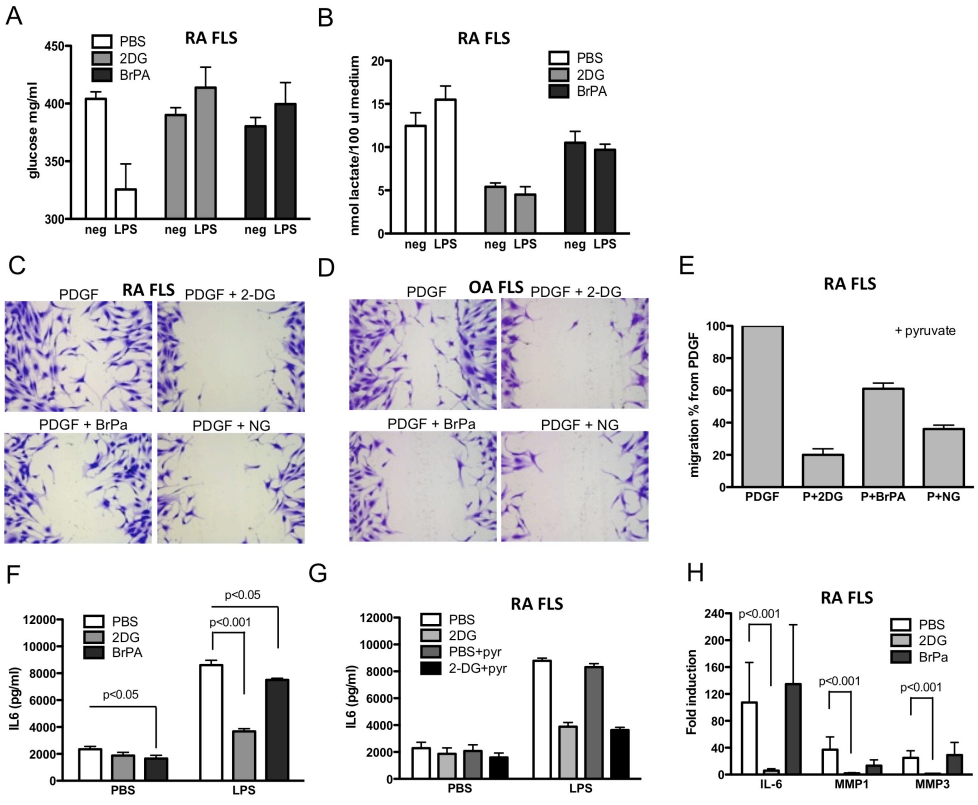

Supplementary Figure 5. Effect of glycolytic inhibition on FLS function. (A) Glucose and **(B)** lactate in supernatants 24hrs after LPS stimulation in the presence or absence of glycolytic inhibitors (2-DG: 50mM in PBS, BrPa: 25uM in PBS). **(C)** RA FLS and **(D)** OA FLS were grown to a confluent monolayer in a 6-well plates and a wounded area was generated with 1ml micropipette tip. Cells were then grown in the presence of PDGF (10ng/ml) with 2-DG and BrPA, or NG medium. Pictures were taken after 36 hrs. Representative image of one RA FLS and OA FLS after crystal violet staining in the migration scratch assay under the above conditions is shown. **(E)** FLS were assessed for migration as described in Methods. Quantification of migration in medium with pyruvate (as the average of relative area between margins in 4 different fields from 2 different RA FLS cell lines) is shown in the graph. **(F)** OA FLS were cultured in the presence of LPS

(1μg/mL) with or without pretreatment with 2-DG (50mM) or BrPa (25μM) for 24 hrs. Supernatant from OA cell cultures were analyzed for secretion of IL-6. Results are pooled from 4 different cell lines. **(G)** RA FLS were cultured in the presence of LPS (1μg/mL) with or without pretreatment with 2-DG (50mM) or BrPa (25μM) for 24 hrs and RNA isolation of RA FLS were prepared after 24hrs of LPS stimulation. **(H)** IL-6, MMP1 and MMP3 expression were analyzed by qPCR. Results are pooled from 4 different cell lines.

Supplementary Figure 6

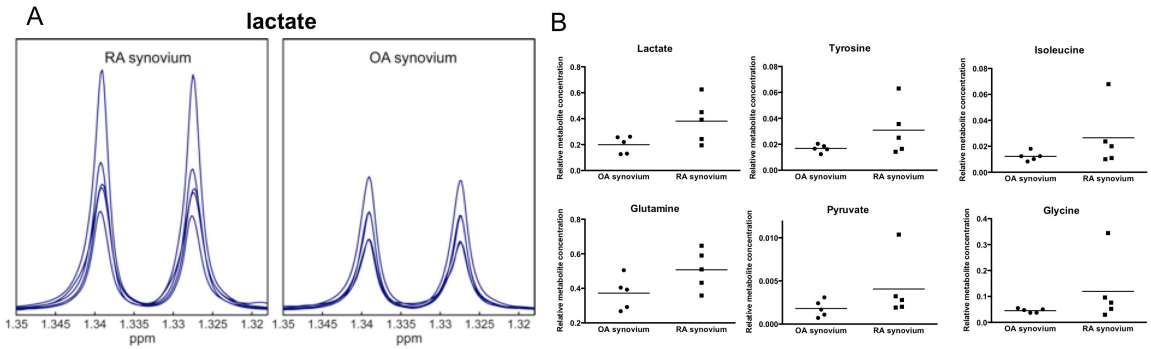

Supplementary Figure 6. Glycolytic metabolite profile in arthritic synovium. **(A)** ^{1}H-MRS lactate spectra obtained from OA and RA synovium. **(B)** Representation of select metabolites quantification obtained from 5 OA and 5 RA synovium samples by ^{1}HNMR.

Supplementary Figure 7

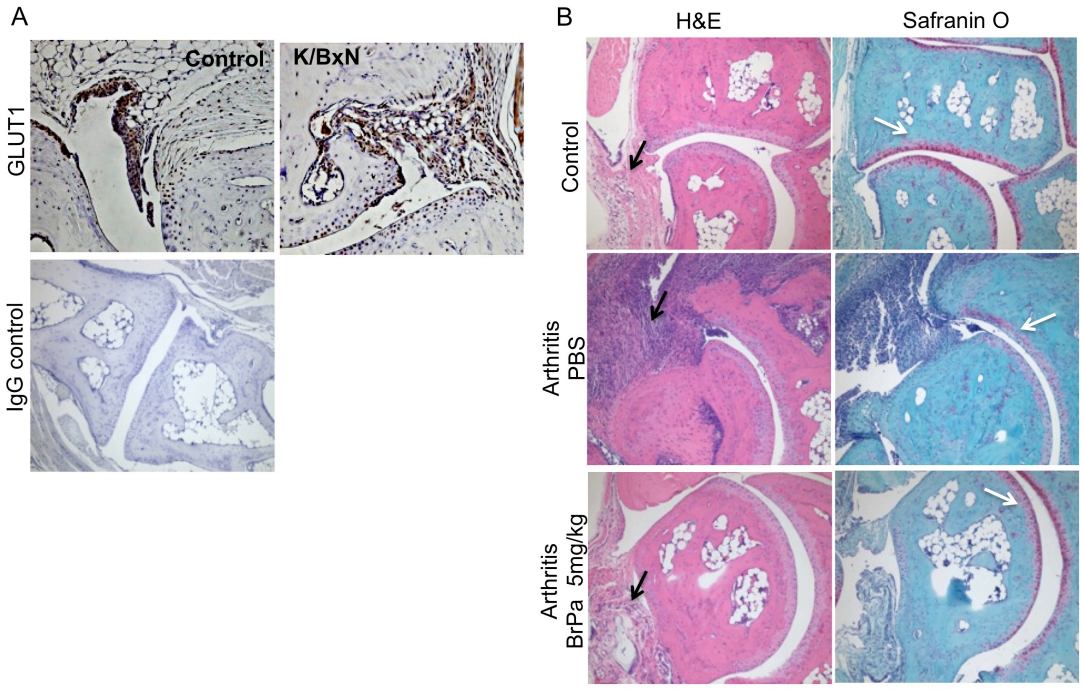

Supplementary Figure 7. Glycolytic inhibition decreases histologic scores and inflammatory mediators in the K/BxN model. (A) Representative GLUT1 stained section of control ankle and arthritic ankle on day 7 of arthritis induction and IgG control (200x magnification). **(B)** Representative H&E and Safranin O stained sections of ankle joints on day 7 of arthritis induction in control joints, and PBS and BrPA (5mg/kg)-treated mice after K/BxN injection (200x magnification). Black arrows in H&E stained sections indicate joint inflammation and white arrows in Safranin O stained sections highlight cartilage damage that was reduced in BrPa-treated ankles.

REFERENCES

1. Tiziani S, *et al*. (2009) Metabolomic profiling of drug responses in acute myeloid leukaemia cell lines. (Translated from eng) *PLoS One* 4(1):e4251 (in eng).
2. Wu H, Southam AD, Hines A, & Viant MR (2008) High-throughput tissue extraction protocol for NMR- and MS-based metabolomics. (Translated from eng) *Anal Biochem* 372(2):204-212 (in eng).
3. Ludwig C & Gunther UL (2011) MetaboLab--advanced NMR data processing and analysis for metabolomics. (Translated from eng) *BMC Bioinformatics* 12:366 (in eng).
4. Dieterle F, Ross A, Schlotterbeck G, & Senn H (2006) Probabilistic quotient normalization as robust method to account for dilution of complex biological mixtures. Application in 1H NMR metabonomics. (Translated from eng) *Anal Chem* 78(13):4281-4290 (in eng).
5. Ludwig C EJ, Lodi A, Tiziani S, Manzoor SE, et al (2012) Birmingham Metabolite Library: a publicly accessible database of 1-D H-1 and 2-D H-1 J-resolved NMR spectra of authentic metabolite standards (BML-NMR). *Metabolomics* 8:8-18.
6. Psychogios N, *et al*. (2011) The Human Serum Metabolome. (Translated from English) *PLoS One* 6(2) (in English).
7. Mookerjee SA, Goncalves RL, Gerencser AA, Nicholls DG, & Brand MD (2015) The contributions of respiration and glycolysis to extracellular acid production. (Translated from eng) *Biochim Biophys Acta* 1847(2):171-181 (in eng).
8. Fridman A, *et al*. (2013) Cell cycle regulation of purine synthesis by phosphoribosyl pyrophosphate and inorganic phosphate. (Translated from eng) *Biochem J* 454(1):91-99 (in eng).
9. Saha A, *et al*. (2014) Akt phosphorylation and regulation of transketolase is a nodal point for amino acid control of purine synthesis. (Translated from eng) *Mol Cell* 55(2):264-276 (in eng).
10. Boss GR & Pilz RB (1985) Phosphoribosylpyrophosphate synthesis from glucose decreases during amino acid starvation of human lymphoblasts. (Translated from eng) *J Biol Chem* 260(10):6054-6059 (in eng).
11. Guma M, *et al*. (2009) Caspase 1-independent activation of interleukin-1beta in neutrophil-predominant inflammation. (Translated from eng) *Arthritis Rheum* 60(12):3642-3650 (in eng).